Supporting Information

Platelet-derived nanomotor coated balloon for atherosclerosis combination therapy

Yangyang Huang‡[a], Ting Li‡[a], Wentao Gao[b], Qi Wang[a], Xiaoyun Li[a], Chun Mao[a], Min Zhou*[b], Mimi Wan*[a], and Jian Shen[a]*

[a]National and Local Joint Engineering Research Center of Biomedical Functional Materials, School of Chemistry and Materials Science, Nanjing Normal University, 210023, P. R. China

[b]Department of Vascular Surgery, Nanjing Drum Tower Hospital, The Affiliated Hospital of Nanjing University Medical School, 210008, P. R. China

‡These authors contributed equally to this work.

Corresponding Author

*(C.M) maochun@njnu.edu.cn
*(M.Z) zhouminnju@126.com
*(M.M.W) wanmimi@njnu.edu.cn

Keywords: atherosclerosis, drug-coated balloons, nanomotors, deep-penetration, photothermal elimination

Experimental details

Cy5.5 modificaiton of nanomotors

The steps for the modification of Cy5.5 on nanomotor are as follows. [1] 50 mg JAMS was dispersed in 10 mL of $NaHCO_3$ solution (0.1 M), then 1.25 mL of dimethylsulfoxide (DMSO) solution (Cy5.5-NHS, 1 mg mL^{-1}) was added and stirred overnight under dark. The reacted solution was dialyzed in distilled water for 48 hours to remove DMSO and unreacted Cy5.5-NHS. Then the dialyzed product was freeze-dried to obtain Cy5.5 modified nanomotors.

Analysis of the antibody modification

Through labelled avidin-biotin technique, phycoerythrin (PE)-streptavidin can selectively combined with the antibody, so it was chosen to confirm the successful modification of vascular cell adhesion molecule-1 (anti-VCAM-1) antibody.[2] Under the excitation wavelength of 488 nm, PE-streptavidin can release a strong fluorescence emission peak at 575 nm, so the PE-streptavidin was used to combine with the antibody modified material to determine whether the modification was successful. First, 0.1 mL of the PE-streptavidin (Biolegend, US) solution (20 μg mL^{-1}) was added to the suspension containing the MJAMS/PTX/aV nanomotor, and incubated for 1 h. After the incubation, the supernatant was separated and discarded by centrifugation (10000 rpm, 10 min). Then deionized water (DW) (1 mL) was added to wash off the dissociative PE-streptavidin. After washing for 3 times, the material was dispersed into DW (1 mL) and detected by the fluorescence spectrophotometer.

Test of calibration curves of paclitaxel

The calibration curve of paclitaxel at different concentrations was determined as follows. First, the standard paclitaxel solutions at different concentrations (2, 4, 6, 8, 10, 12, 14, 18 μg mL^{-1}) were prepared by using phosphate buffer solution (PBS) containing 1% Tween 80 and Tween 20, and then absorption of the standard paclitaxel solution was measured by UV spectrophotometer at 232 nm. The standard solution prepared with PBS solution containing 1% Tween 80 and Tween 20 is intended to be consistent with the actual drug release solution of the nanomotor.

Test of hemolysis and morphological changes of RBCs

First, the RBCs of rabbit blood was separated from serum by centrifugation (2500 rpm, 15 min) and washed with PBS solution for four times until the supernatant contained no plasma or platelets. Then, the RBCs was diluted to PBS solution to be prepared into 2% RBCs suspension. Next, 0.1 mL of solution of different samples (Fe_3O_4/MS, MS, MS/PTX, JAMS, JAMS/PTX, MJAMS/PTX, MJAMS/PTX/aV) (1mg mL^{-1}) was added into 2% RBCs suspension individually and incubated for 3 h at 37 ℃, and then centrifuged at 2500 rpm for 15 min to acquire the supernatant liquid. DW and PBS solution were denoted as positive and negative controls.The UV-visible spectrophotometer was used to detect the UV absorption of the liquid at 541 nm. The hemolysis was calculated according to the following formula:

$$\text{Hemolysis (\%)} = (OD_{sample} - OD_{negative}) \times 100\% / (OD_{positive} - OD_{negative}),$$

in which OD_{sample} refers to the absorption value of the sample liquid, and $OD_{negtive}$ and $OD_{positive}$ refer to absorption value of the PBS control group and DW control group, respectively.

The morphological changes of RBCs were observed and recorded with a camera (Olympus Group, Japan).

In vitro cell viability

The viability of human umbilical vein endothelial cells (HUVECs) cultured with different materials (Fe_3O_4, Fe_3O_4/MS, MS, JAMS, MJAMS/PTX, MJAMS/PTX/aV) was detected by the MTT assay. The HUVECs (1×10^5 cells/mL) were pre-cultured in 96-well plates at 37 ℃ overnight in an incubator with 5% CO_2. After discarding the previous medium, the cells were treated with 200 μL medium containing different materials (0.2 mg mL^{-1}), and pure medium treated cells were used as control group. After incubating for 24 h, 50 μL of MTT solution (5 mg mL^{-1}) was injected into the wells and incubated without light for 4 h. Then 150 μL of DMSO was added into the wells to dissolve the purple crystal after removing the previous medium. After 10 min of shaking, the absorbance of solution in each well was tested by using the UV-visible spectrophotometer at 570 nm.

FITC modification of JAMS

30 mg JAMS was dispersed in 30 mL of water and 30 mL of anhydrous ethanol, and 100 μL of APTES and 400 μL of FITC (0.25 mg mL^{-1}) were added into the solution. The reaction was carried out at 40 °C for 24 h under dark conditions. After the reaction, the obtained FITC-modified nanomotor was washed by centrifugation with water and ethanol at 10,000 rpm for three times, respectively.[3,4]

Evaluation of penetration ability of the MJAMS/PTX/aV nanomotor

To simulate atherosclerotic plaque, thrombus was made by heating the mixture which was consist of 9 mL of blood and 0.138 g gelatin under 50 ℃ for 1 h. To study the penetrating effect of the nanomotor under static condition, the thrombus was immersed in JAMS solution (0.1 mg mL^{-1}) and MJAMS (0.1 mg mL^{-1}) respectively and treated with or without near-infrared (NIR) laser for 10 min at 2.0 W cm^{-2}. Then the dynamic condition of the penetrating effect of the material was also evaluated by simulating the condition of thrombus under real blood flow. All the thrombus were weighed and Pt concentrations were quantified by inductively coupled plasma emission spectrometer (ICP).

Intracellular transfer

HUVECs (1×10^5 cells/mL) and RAW264.7 (1×10^5) on coverslip were pre-cultured in the medium for 12 h. Then MJAMS/aV/FITC (50 μg mL^{-1}) was added into the HUVECs and treated with or without NIR for 5 min at 2.0 W cm^{-2}. After incubation for 2 h, the coverslips of HUVECs and RAW264.7 were incubated together and treated with or without NIR for 5 min at 2.0 W cm^{-2}. After incubation for 12 h, the cells were washed with PBS solution and dyed with 4',6-diamidino-2-phenylindole (DAPI) before observation by the confocal laser scanning microscope.[5]

Additional figures

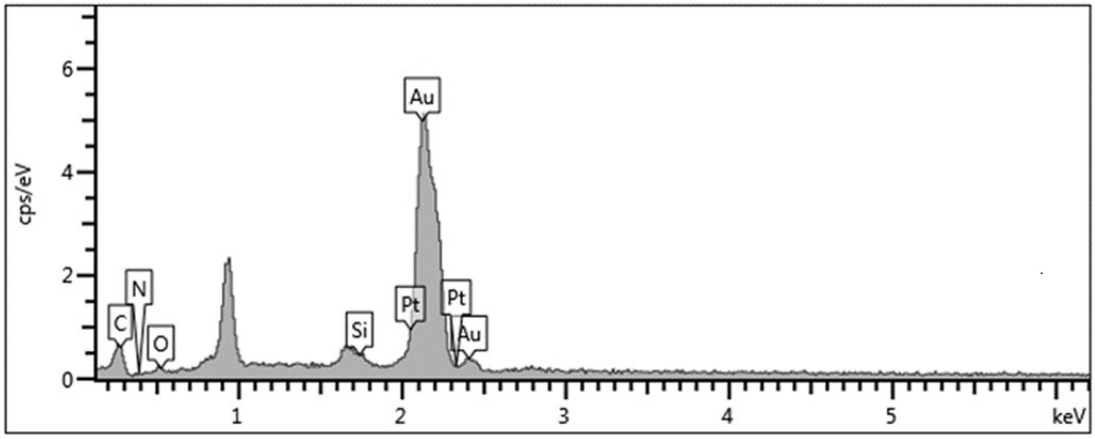

Fig. S1. Energy dispersive spectrometer spectrum of JAMS.

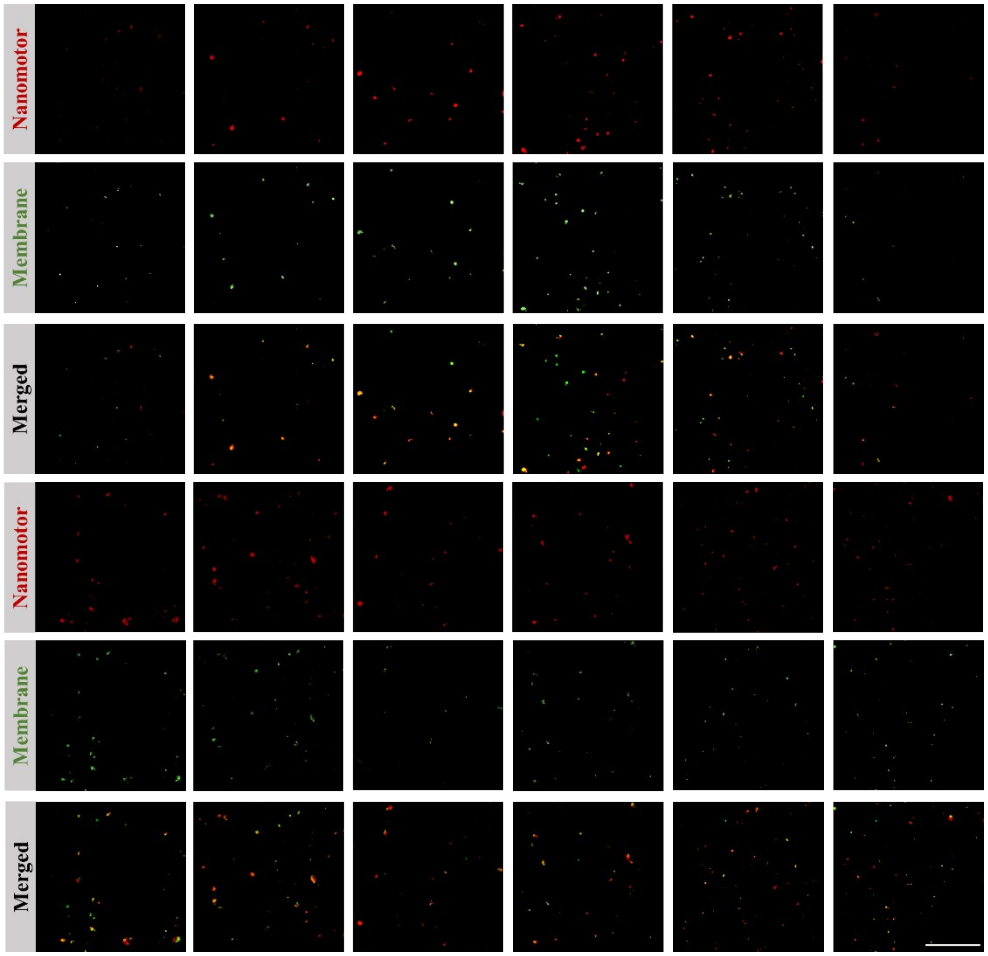

Fig. S2. CLSM images of DiO-labelled platelet membrane (green) coated cy5.5-labelled nanomotors (red) (Scale bar: 50 μm).

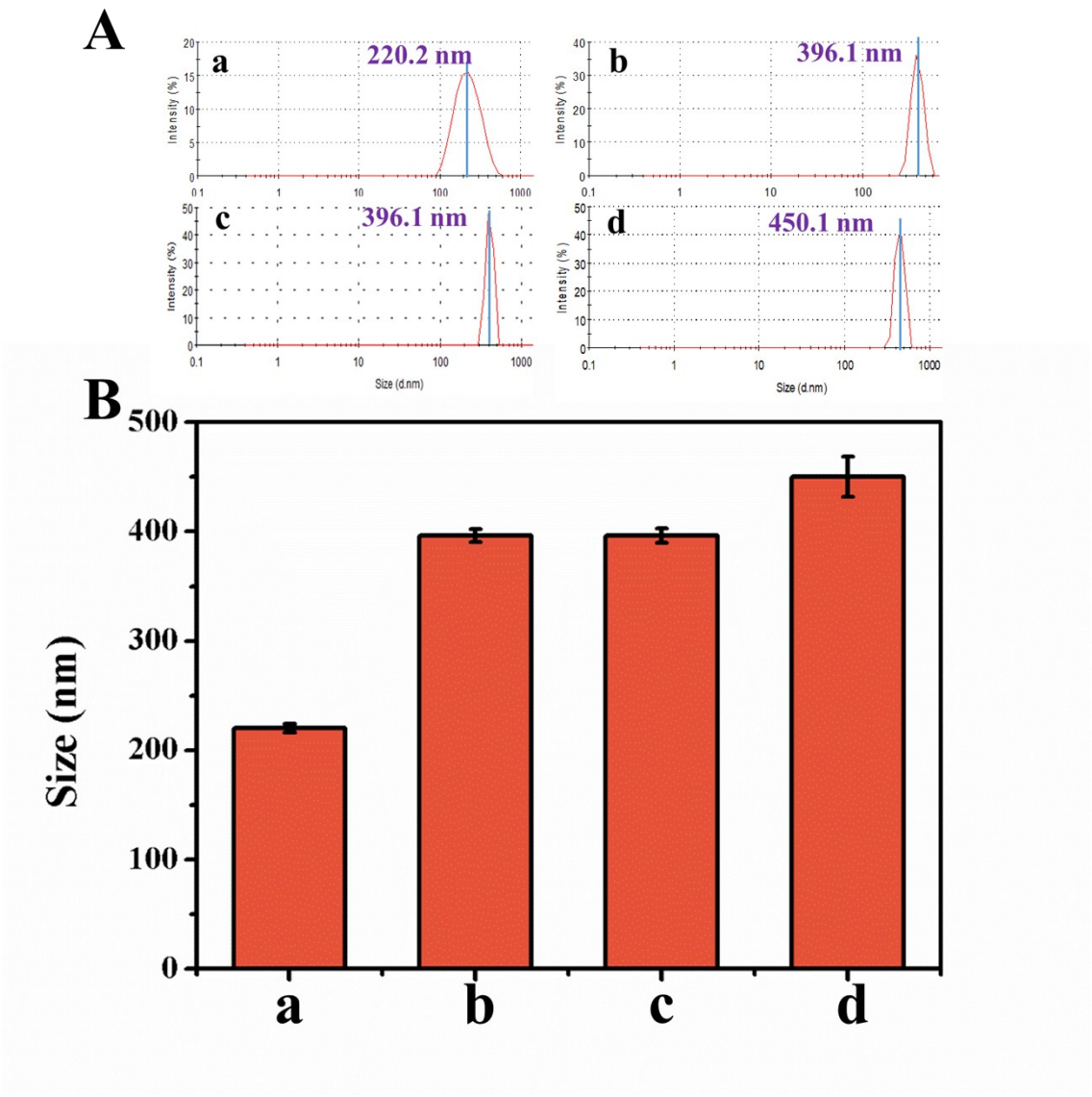

Fig. S3. Size analysis of different materials. (A) DLS curves of (a) Fe_3O_4, (b) Fe_3O_4/MS, (c) MS, and (d) JAMS, and (B) their corresponding particle sizes.

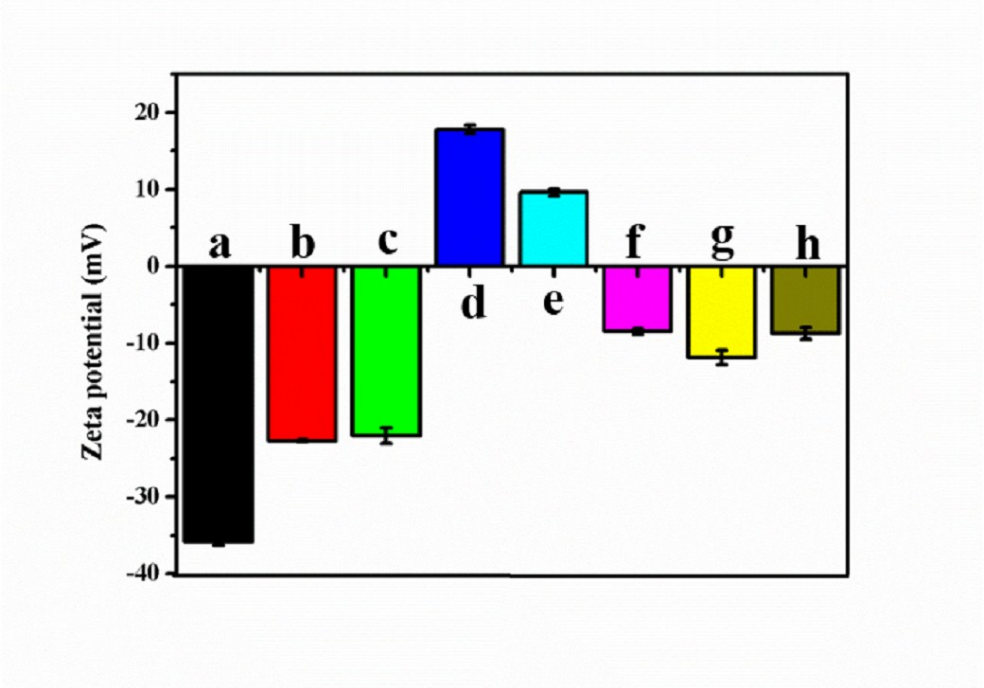

Fig. S4. Zeta potential of (a) Fe_3O_4, (b) Fe_3O_4/MS, (c) MS, (d) AMS, (e) JAMS, (f) JAMS/PTX, (g) MJAMS/PTX, and (h) MJAMS/PTX/aV.

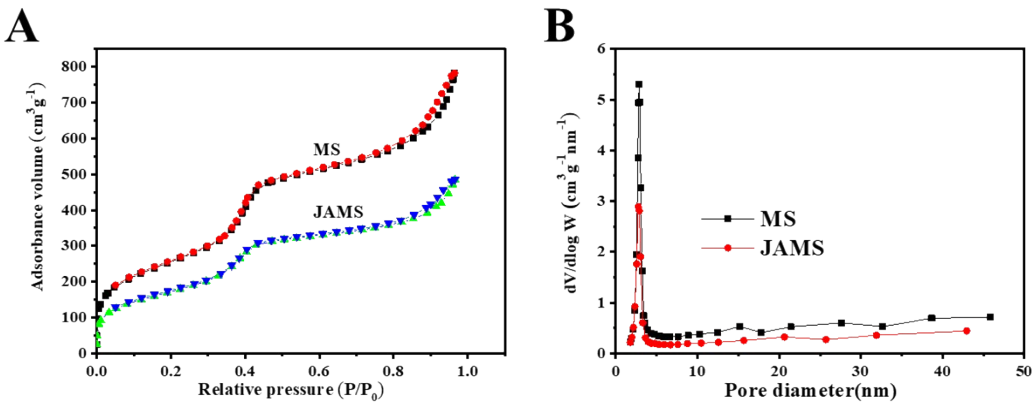

Fig. S5. (A) Nitrogen adsorption−desorption isotherms of MS and JAMS; (B) Pore size distribution of MS and JAMS.

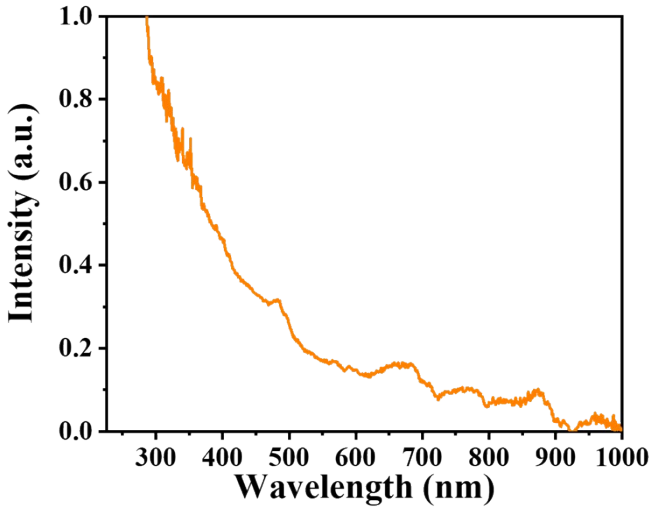

Fig. S6. UV-Vis-NIR spectrum of JAMS/PTX.

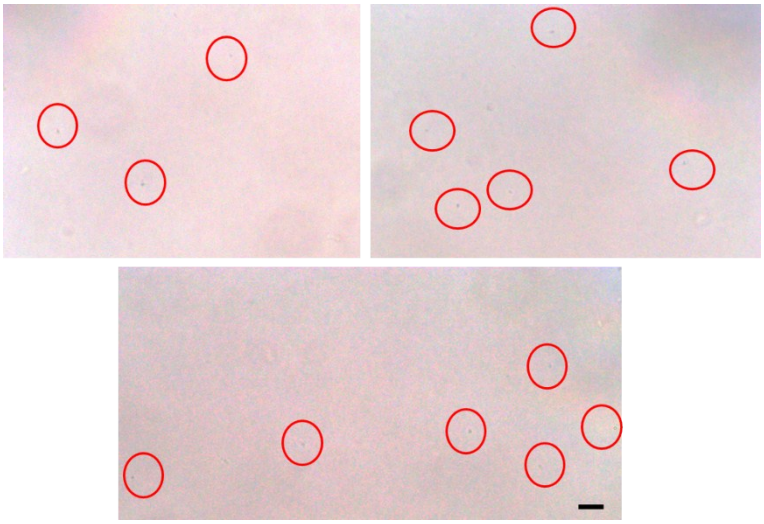

Fig. S7. Images of MJAMS/PTX/aV nanomotor under optical microscope (Scale bar: 10 μm).

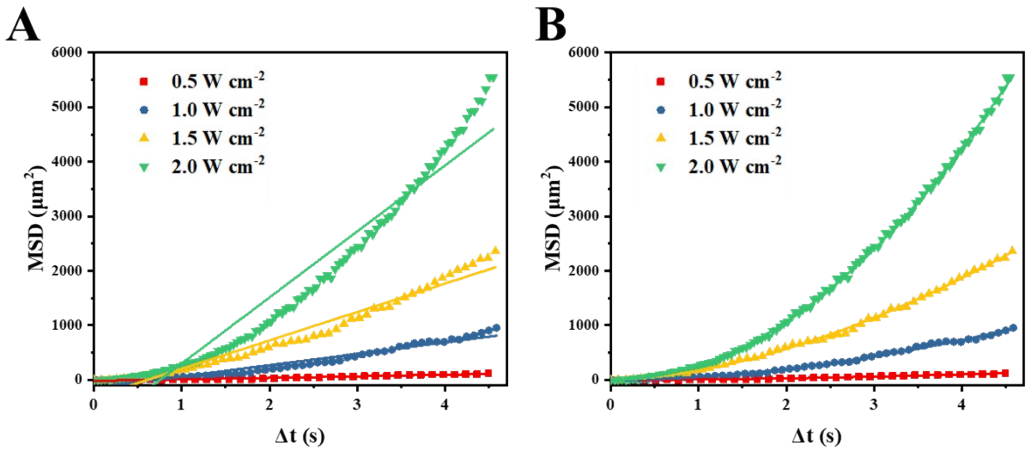

Fig. S8. (A) Linear (y = ax + b) and (B) power function ($y = ax^b$) fitting for MSD plots of MJAMS/PTX/aV under different NIR laser power densities.

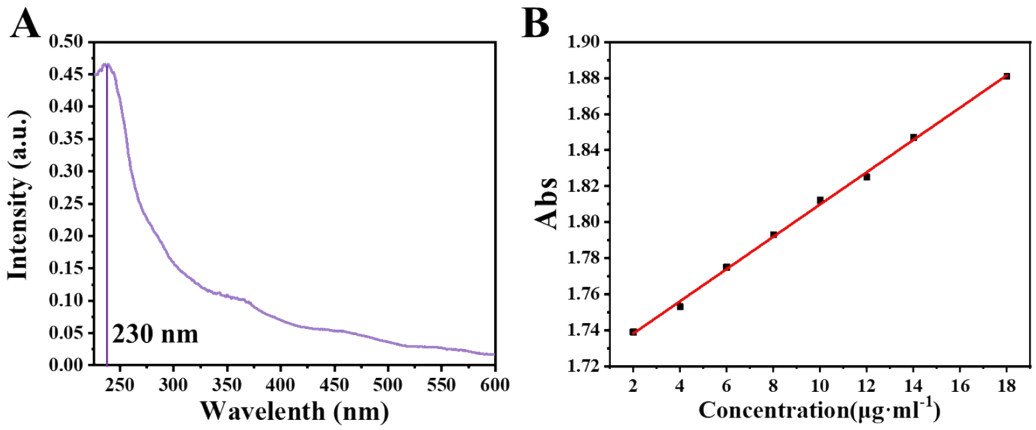

Fig. S9. (A) UV-Vis spectra of paclitaxel; (B) Calibration curve of PTX solution.

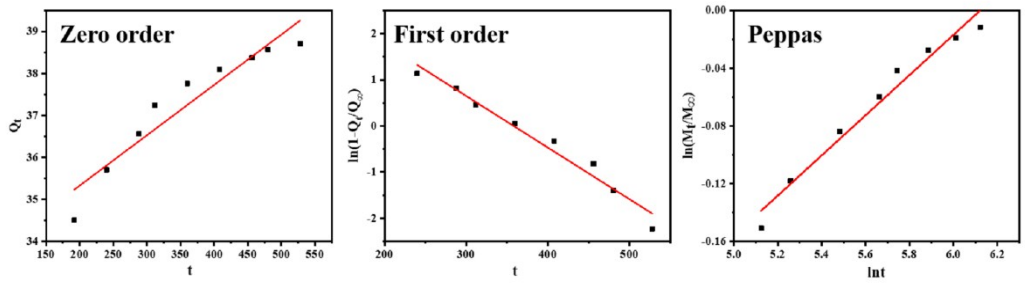

Fig. S10. Release profile of MS/PTX fits to zero, first and Peppas models for PTX.

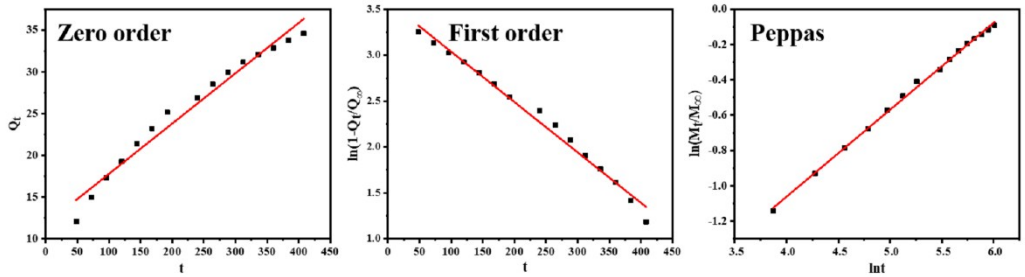

Fig. S11. Release profile of JAMS/PTX fits to zero, first and Peppas models for PTX.

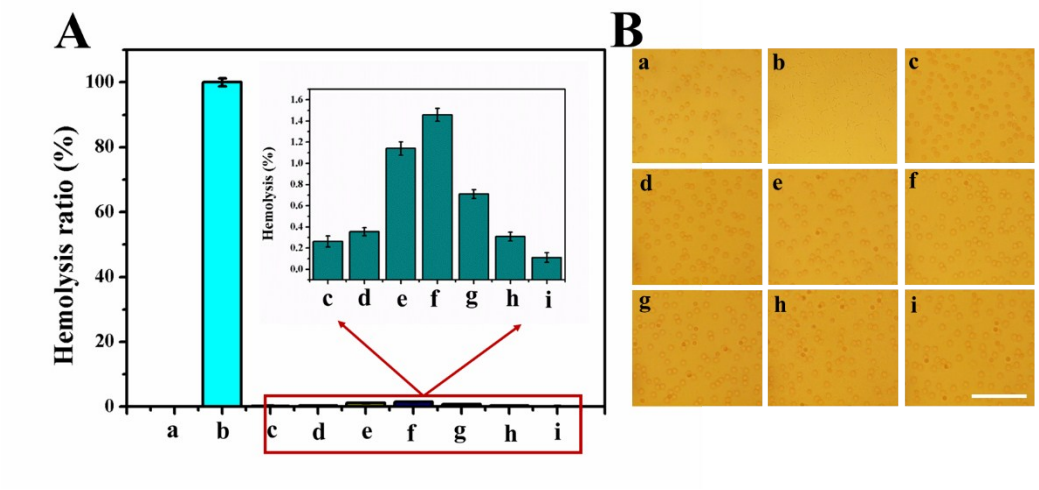

Fig. S12. Biocompatibility tests of materials in blood. (A) Hemolysis and (B) optical images obtained from RBCs of (a) negative control, (b) positive control, (c) Fe_3O_4/MS, (d) MS, (e) JAMS, (f) MS/PTX, (g) JAMS/PTX, (h) MJAMS/PTX, and (i) MJAMS/PTX/aV (Scale bar: 50 μm).

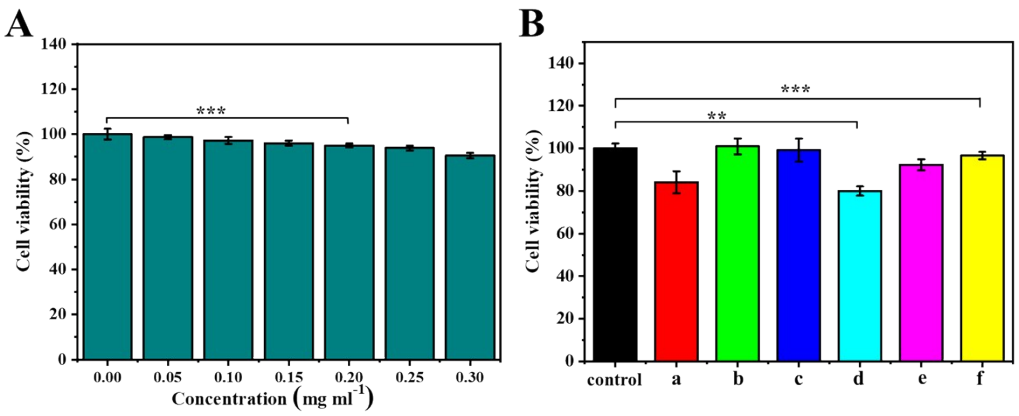

Fig. S13. Biocompatibility tests of the nanomotor. (A) Cell viability of RAW264.7 after incubation with different concentrations of MJAMS/PTX/aV for 24 h. (B) Cell viability of HUVECs cultured with (a) Fe_3O_4, (b) Fe_3O_4/MS, (c) MS, (d) JAMS, (e) MJAMS/PTX and (f) MJAMS/PTX/aV for 24 h. Asterisk (*) denotes statistical significance between bars (*p<0.05, **p<0.01, ***p<0.001) using one-way ANOVA analysis. Experimental data are mean+/−s.d. of samples in a representative experiment (n = 3).

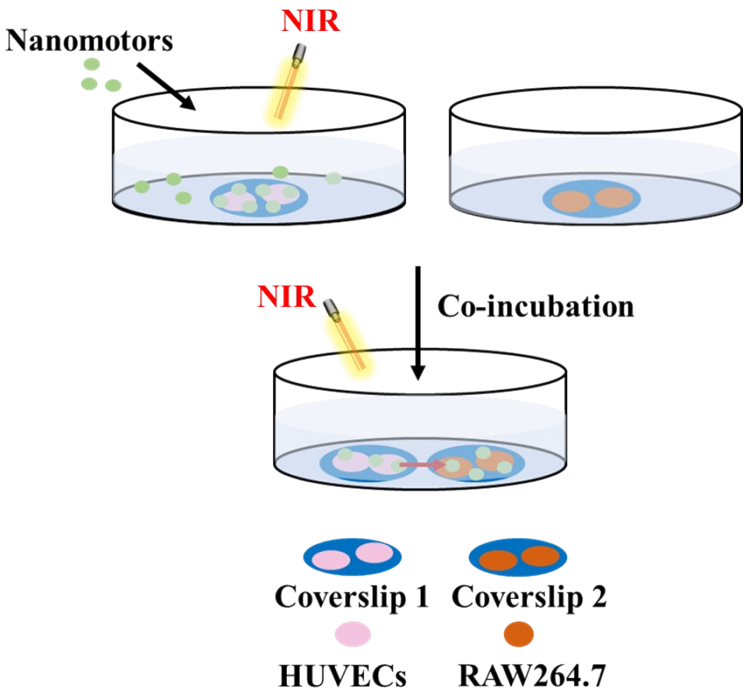

Fig. S14. Schematic illustration of the process of MJAMS/aV/FITC transfer experiment from HUVECs to RAW264.7.

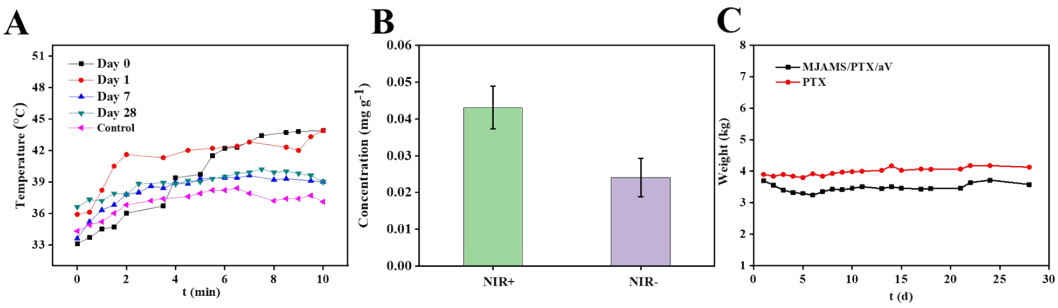

Fig. S15. (A) Temperature profile of the thermal image on day 0, 1, 7, and 28 of the MJAMS/PTX/aV group; (B) ICP results of Pt content within the carotid artery of the rabbits treated with or without NIR laser; (C) Body weight of the rabbits during 28 days.

Additional tables

Table S1. Summary of current researches of coatings for DCB.

Year	Excipient/ Nanoparticle	Drug	Therapy method	*In vivo* model	Ref
2011	Iopromide	Paclitaxel	Drug	Pig	*6*
2011	BHTC	Paclitaxel	Drug	Pig	*7*
2012	Urea	Paclitaxel	Drug	Human	*8*
2015	Dextran sulfate	Paclitaxel	Drug	-	*9*
2016	PEO	Paclitaxel	Drug	-	*10*
2013	Phospholipid encapsulated sirolimus nanocarrier	Sirolimus	Drug	Rabbit	*11*
2013	*nab*-rapamycin	Rapamycin	Drug	Pig	*12*
2017	Silica-gold nanoparticles	-	Photo-thermal (PTT)	Human	*13*
2018	PLGA-Eudragit nanoparticle	Polyphenol	Drug	-	*14*
2019	PLGA nanoparticle	Bovine serum albumin	Drug	-	*15*
2020	MJAMS/PTX/aV nanomotor	Paclitaxel	PTT and drug	Rabbit	*This work*

Table S2. Physicochemical properties of MS and JAMS.

Samples	S_{BET} (m^2 g^{-1},C)	V (cm^3 g^{-1})	D (nm)
MS	930	1.27	3.2
JAMS	635	0.79	3.2

Table S3. Linear fitting parameters for MSD plot of MJAMS/PTX/aV under different laser power densities (y = ax+ b).

Laser power density (W cm^{-2})	R^2	a	b
0.5	0.9568	28.19	-18.50
1.0	0.9447	208.87	-146.13
1.5	0.9590	521.25	-316.99
2.0	0.9367	1211.57	-909.15

Table S4. Parabolic fitting parameters for MSD plot of MJAMS/PTX/aV under different laser power densities ($y = ax^2 + bx + c$).

Laser power density ($W\ cm^{-2}$)	R^2	a	b	c	$V_{(MSD)}$	$V_{(actual)}$
0.5	0.9872	4.21	9.26	-4.74	2.05	2.28
1.0	0.9950	40.02	15.50	-8.72	6.33	5.58
1.5	0.9988	88.37	117.35	-15.13	9.40	10.08
2.0	0.9999	264.80	7.78	-5.69	16.27	15.11

Table S5. Power function fitting parameters for MSD plot of MJAMS/PTX/aV under different laser power densities ($y = ax^b$).

Laser power density ($W\ cm^{-2}$)	R^2	a	b
0.5	0.9871	9.40	1.70
1.0	0.9951	56.13	1.85
1.5	0.9986	174.32	1.71
2.0	0.9995	268.80	1.99

Table S6. Parameters and coefficients obtained for zero order release kinetic model $Q_t = K_0 t$, first order release kinetic model $ln(1-Q_t/Q_\infty) = lnQ_\infty - K_1 t$, and Peppas release kinetic model $M_t/M_\infty = a \times t^b$ fitted to PTX released from MS/PTX.

Release models	Release parameters	Value
Zero order	K_0	0.012
	R^2	0.906
First order	K_1	0.011
	R^2	0.969
Peppas	a	0.002
	b	0.139

	R^2	0.972

Table S7. Parameters and coefficients obtained for zero order release kinetic model $Q_t=K_0t$, first order release kinetic model $ln(1-Q_t/Q_\infty)=lnQ_\infty-K_1t$, and Peppas release kinetic model $M_t/M_\infty = a \times t^b$ fitted to PTX released from JAMS/PTX.

Release models	Release parameters	Value
Zero order	K_0	0.060
	R^2	0.971
First order	K_1	0.005
	R^2	0.988
Peppas	a	0.002
	b	0.492
	R^2	0.998

Table S8. Parameters and coefficients obtained for zero order release kinetic model $Q_t=K_0t$, first order release kinetic model $ln(1-Q_t/Q_\infty)=lnQ_\infty-K_1t$, and Peppas release kinetic model $M_t/M_\infty = a \times t^b$ fitted to PTX released from MJAMS/PTX.

Release models	Release parameters	Value
Zero order	K_0	0.075
	R^2	0.986
First order	K_1	0.005
	R^2	0.992
Peppas	a	0.002
	b	0.677
	R^2	0.997

References

1 Z. X. Lu, F. Y. Huang, R. Cao, G. H. Tan, G. H. Yi, N. Y. He, L. F. Xu, L. M. Zhang, *ACS Appl. Mater. Interfaces*, 2018, **10**, 26028-26038.

2 H. Yang, L. Zhang, X. Y. Xiong, Y. Y. Liu, *J. Control. Release*, 2011, **152**, e192-e229.

3 H. Y. Liu, F. J. Chen, P. X. Xi, B Chen, L. Huang, J. Cheng, C. W. Shao, J. Wang, D. C. Bai, Z. Z. Zeng, *J. Phys. Chem. C*, 2011, **115**, 18538–18544.

4 Y. Zhou, J. Ding, T. X. Z. Liang, E. S. Abdel-Halim, L. P. Jiang, J. J. Zhu, *ACS Appl. Mater. Interfaces*, 2016, **8**, 6423-6430.

5 Q. Zhou, S. Q. Shao, J. Q. Wang, C. H. Xu, J. J. Xiang, Y. Piao, Z. X. Zhou, Q. S. Yu, J. B. Tang, X. R. Liu, Z. H. Gan, R. Mo, Z. Gu, Y. Q. Shen, *Nat. Nanotechnol.*, 2019, **14**, 799-809.

6 M. Krzysztof, T. Armando, A. Michael S, C. Gerard, Yi, G. Hua, T. Troels, S. Mark, M. Jennifer, G. William, V. Renu, G. Juan, K. Grzegorz L, *EuroIntervention*, 2011, **7**, 362-368.

7 P. W. Radke, M. Joner, A. Joost, R. A. Byrne, S. Hartwig, G. Bayer, K. Steigerwald, E. Wittchow, *EuroIntervention*, 2011, **7**, 730-737.

8 S. Cassese, R. A. Byrne, I. Ott, G. Ndrepepa, M. Nerad, A. Kastrati, M. Fusaro, *Circ. Cardiovasc. Interv.*, 2012, **5**, 582-589.

9 S. Lamichhane, J. Anderson, T. Remund, P. Kelly,3 G. Mani, *J. Biomed. Mater. Res. Part B*, 2016, **104B**, 1416-1430.

10 J. A. Anderson, S. Lamichhane, T. Remund, P. Kelly and G. Mani, *Acta Biomater.*, 2016, **29**, 333-351.

11 P.A. Lemos, V. Farooq, C.K. Takimura, P.S. Gutierrez, R. Virmani, F. Kolodgie, U.

Christians, A. Kharlamov, M. Doshi, P. Sojitra, H.M. van Beusekom, P.W. Serruys, *EuroIntervention*, 2013, **9**, 148-156.

12 W. J. Gasper, C. A. Jimenez, J. Walker, M. S. Conte, K. Seward, C. D. Owens, *Circ. Cardiovasc. Interv.*, 2013, **6**, 701-709.

13 A. N. Kharlamov, , J. A. Feinstein, J. A. Cramer1, J. A. Boothroyd, E. V. Shishkina, V. Shur, *Future Cardiol.*, 2017, **13**, 345-363.

14 Ta. R. Dugas, G. Brewer, M. Longwell, T. Fradella, J. Braun, C. E. Astete, M. H. Jennings, C. M. Sabliov, *J. Biomed. Mater. Res. Part B*, 2018, **107B**, 646-651.

15 R. Iyer, A. E. Kuriakose, S. Yaman, L. C. Su, D. Shan, J. Yang, J. Liao, L. Tang, S. Banerjee, H. Xu, K. T. Nguyen, *Int. J. Pharm.*, 2019, **554**, 212-223.